Interannual Variability of Winter Rainfall in Upper Myanmar

Kyaw Than Oo[1,2]

[1]Nanjing University of Information Science and Technology, Nanjing, China
[2]Aviation Weather Services, Myanmar Air Force, Myanmar

*Corresponding author: kyawthanoo34@outlook.com　ⓘD

Abstract: Upper Myanmar region, roughly located between 21˚00' N and 28˚30' N latitude and 92˚ 10' E and 101˚ 11' E longitude, is the place where the winter cold season contributes ~2% of the annual total rainfall. The rainfall associated with Western disturbances is small in quantum but veritably important for the cold season crops, maintaining the glaciers over the Putao region, hydropower generation for the whole country and hazard of Jade mining of the Upper Myanmar area. This study aims to find interannual variability and related ocean-atmospheric pattern link with Upper Myanmar cold season rainfall by using great-resolution reanalysis data (ERA5) during 1990-2020. Correlation analysis to test the validation of ERA5 gridded data with the observed data from 25 stations across Myanmar, showed a strong correlation value in the same period that enough reliable for best analysis results. An anomalous anticyclonic (cyclonic) circulation persists over the southern part of the Bay of Bengal and South China sea during wet (dry) years. Also, the warming over the Indian Ocean and the cooling over the Tibetan plateau region correspond to south-north transport of moisture, ensuing in positive rainfall anomalies over the study region during winter. The wide patches of strong negative (positive) correlation are found over the Pacific Ocean, the Atlantic Ocean, Mediterranean Sea (MED), Arabian Sea (ARS), and Red Sea (RED) during wet (dry) years. The link implies that NPO, SPO, and MED have an impact on the winter rainfall inter-annual variability. In addition, the cooling (warming) over the Indochina and western Pacific regions influences the Hadley and Walker circulation bringing above (below) normal rainfall, respectively, over Upper Myanmar. The reply of indices (PO, MED, NINO3.4, IOD, and WDs) on winter rainfall, necessary to further investigation. The complete analysis of winter rainfall aids in the understanding of past extreme events as well as the forecasting and monitoring of drought and floods in Upper Myanmar.

Keywords: Myanmar rainfall, Sea surface temperature, Western disturbances, Winter rainfall

1. Introduction

Myanmar is situated in a tropical climate region. It is adjacent to China on the North, India and Bangladesh on the West, Thailand and Laos PDR on the South, and there is the Bay of Bengal and the Andaman Sea on the South. The climate of Myanmar is determined mainly by its geographical position. It lies in the South of the great Asiatic continent and to the North of the Indian Ocean. Myanmar is separated from neighboring countries by high mountain walls. In the extreme north lies the great Himalaya Mountain and, the Chin Hills, and the Yoma with an average height of within 6000 ft to 12000 ft, separating Myanmar from India (Zin, 2017). This study will analyze over Upper Myanmar region, where is roughly located between 21˚00' N and 28˚30' N latitude

and 92˚ 10' E and 101˚ 11' E longitude (Figure 1). In the winter season, there is much less amount of rainfall over Myanmar, but the Northern parts of the country receive a considerably higher amount of rainfall than other parts. Myanmar area during March and April and the mean minimum temperature of 40°F (4.4°C) to 50°F (10.0°C) is found to occur in the Northern part of Myanmar during January and February.

Climate variability, substantially the periodic air temperature and rainfall, has entered great attention worldwide. The spatial and temporal variability of rainfall is important from both the scientific and practical points of view. Analysis of spatial-temporal variability of the rainfall has entered considerable attention (Tošić et al., 2013). Nearly like a valve turning off, November sees an unforeseen conclusion of the thunderstorm rains in Upper Myanmar. Clear rainfall generally set in over the country

in Mid-November. The cold season begins over Upper Myanmar in December. In the winter season, low temperatures prevail over the whole country. Clear sky, fine rainfall, low moisture, and temperature and a large quotidian variation of temperatures are the usual features of the rainfall. From about the middle of December, the serenity of the rainfall in Northern Upper Myanmar is broken at intervals by a series of Western disturbances (WDs) which travel Eastwards across Northern Upper Myanmar. The number and character of these disturbances vary, but on average four to six disturbances may be anticipated in each of January and February (Zin, Aung, Zin, Theingi, Elvera, Aung, Han, Oo, Skaland, et al., 2017). The rainfall associated with them is small in quantum but veritably important for the cold season crops of the Upper Myanmar area. Some of the disturbances give rain over the total of upper Myanmar while others confine their conditioning to the extreme North. The cold season rainfall (DJF) over this region plays an important part for (1) cold season crops similar as sticky rice, wheat, peanuts, soybeans, and other variety sap (FAO & AVSI

Foundation, 2019), (2) maintaining the glaciers over the Putao region and Mount Khakaborazi National Park area which is the highest mountain range in Southern Indochina, (3) hydropower generation for the whole country, (4) rainfall of Asia-China high-way, (5) hazard of Jade mining, etc. The cold season rainfall over this region is substantially associated with the passage of mid-latitude synoptic low-pressure systems known as western disturbances that formed/ began over the eastern Mediterranean Sea (MDS) and/ or North Atlantic Ocean (Dimri et al., 2015). The hydro-climatic conditions in Upper Myanmar explosively vary from south to north. Upper Myanmar has unseasonably a lack of meteorological data that permits long-term patterns to be examined and dependable prognostications made of climate changes in the future (N. Sen Roy & Kaur, 2000). Currently, the coupled or atmospheric general rotation models are being extensively used for generating seasonal vaticinations (Nageswararao et al., 2016).
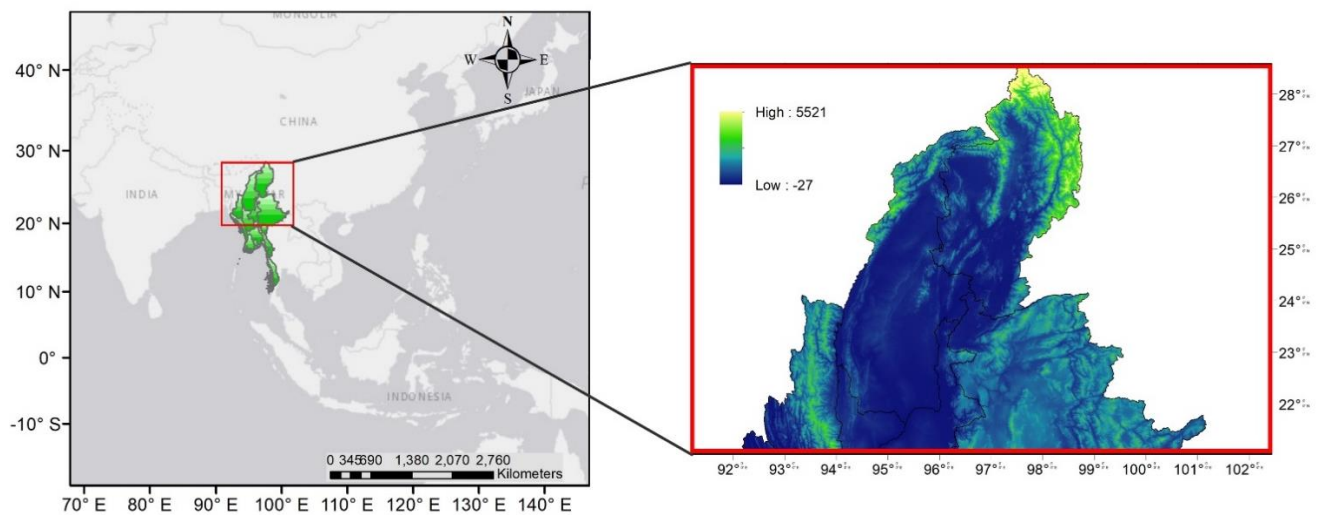

Figure 1: The study area, Myanmar relation to the ocean and landmasses. The inset shows the location of Upper Myanmar with different regions

A well-known atmospheric teleconnection pattern exists in the Northern Hemisphere (NH) midlatitudes, forced by changes in tropical Pacific SSTs associated with ENSO (Bjerknes, 1969; Horel, J. D., 1981). The linear mode of Rossby wave theory helps explain the dynamic relationship between extratropical circulation variation and tropical heating sources (Karoly, 1981). The global forcing that controls the climate of the Northern Hemisphere is El Niño/ Southern Oscillation (ENSO), Arctic Oscillation (AO), and Northern Atlantic Oscillation (NAO). (Cannon et al., 2015) has delved the part of the AO and ENSO on thematic-annual variations in cold season westerly disturbance exertion affecting the Himalayas. In the environment of recent global warming, rainfall variability is linked with Sea Surface Temperature (Dimri et al., 2015). ENSO is the most extensively studied ocean-atmospheric miracle on the variability of the global rainfall (Yadav et al., 2012). The significant link between

ENSO and the climate of Myanmar has been reported in recent decades. Further, the part between ENSO and the summer rainfall has enhance. But winter rainfall has still lack of research. Both the North Atlantic Ocean Dipole (NAD) and NAO can force a dipole SST anomaly pattern by altering the winter latent heat flow (Zhou et al., 2019). Extreme rainfall events have increased since the 1980s. El Nino or La Nina episodes are now more frequently observed around the world after 1972. Several Nino events occurrences occurred between 1981 and 2020. Also, the negative (positive) response of the Indian Ocean Dipole (IOD) has unfavored (favored) the rainfall variability in Myanmar (Sein et al., 2015). The dipole is characterized by the positive (negative) of SST anomalies over the tropical western Indian Ocean and the tropical eastern Indian Ocean. Still, the pronounced warming of the Indian Ocean in recent decades acted as a capacitor to delay and protract the influence of the ENSO (Yang et al., 2007). Therefore, it's necessary to study the whole Indian

Ocean Basin Mode (IOBM) impacts on the interannual variability of the cold season rainfall over south Asia.

The study aims to find the temperature changes in Tibetan Plateau (TP), (India Ocean) IO, Pacific Oceans (PO), Northwest regions of Atlantic Ocean (NWA) and Mediterranean Sea (MED); cyclonic/anticyclonic circulation; and divergent/convergent wind patterns affecting winter rainfall of Upper Myanmar with recently released high-resolution reanalysis data (ERA5). Study analyzes the annual variability of more or less winter rainfall over Upper Myanmar between 1991 and 2020 and presents the physical mechanism of inter-annual variability. Myanmar's economy relies heavily on understanding the variability of winter rainfall since winter harvesting runs from December to February, as well as other economic sectors such as tourism and aviation transportation. Further, it will be useful to comprehend the circumstances of the past extreme events as being the basis for forecasting and monitoring drought and floods over Upper Myanmar.

2. Materials and methods

ERA5 is the fifth generation ECMWF reanalysis for the global climate and weather for the past 4 to 7 decades, reanalysis dataset with the spatial resolution of $0.25° × 0.25°$. Rainfall data taking from GPCP (Global Rainfall Climatology Project) as a reference at a global scale and found that it overestimated deep convection and moisture flux convergence over tropical oceans and land, leading to excessive rainfall (Jiao et al., 2021). The observed rainfall data from 25 meteorological station data across Upper Myanmar for validation were collected from the meteorological stations under-controlled by the Department of Meteorology and Hydrology, Government of Myanmar (DMH).

The large-scale atmospheric parameters such as outgoing long-wave radiation flux (OLR), vertical velocity, wind (u and v components), moisture flux, relative humidity, 2 m Surface Air Temperature (T2M), Convective available potential energy (CAPE), Mean Sea Level Pressure (MSL) and SST are provided by ERA5. The SST indices: NINO3.4, PO, DMI, and IO used in this study were studied from the same ERA5 SST. the average SST anomaly in the region of 5°N to 5°S and 170°W to 120°W (NINO3.4) index is a largely used indicator of ENSO. Alike, the IOD is the difference two SST between the western (50°E–70°E and 10°S–10°N) and the eastern (90°E–110°E and 10°S–10°N) equatorial Indian Ocean (Saji et al., 1999). DMI is an indicator of the intensity results from the calculation of IOD. MED is defined as the averaged SST between 25°N–48°N and 10°W–45°E (Xoplaki et al., 2004). NAD is marked as the averaged SST between (30°N-40°N and 50°W-70°W) IOBM is also defined as the averaged SST between 40°E–110E°; 20°S–20°N (Lu et al., 2019).
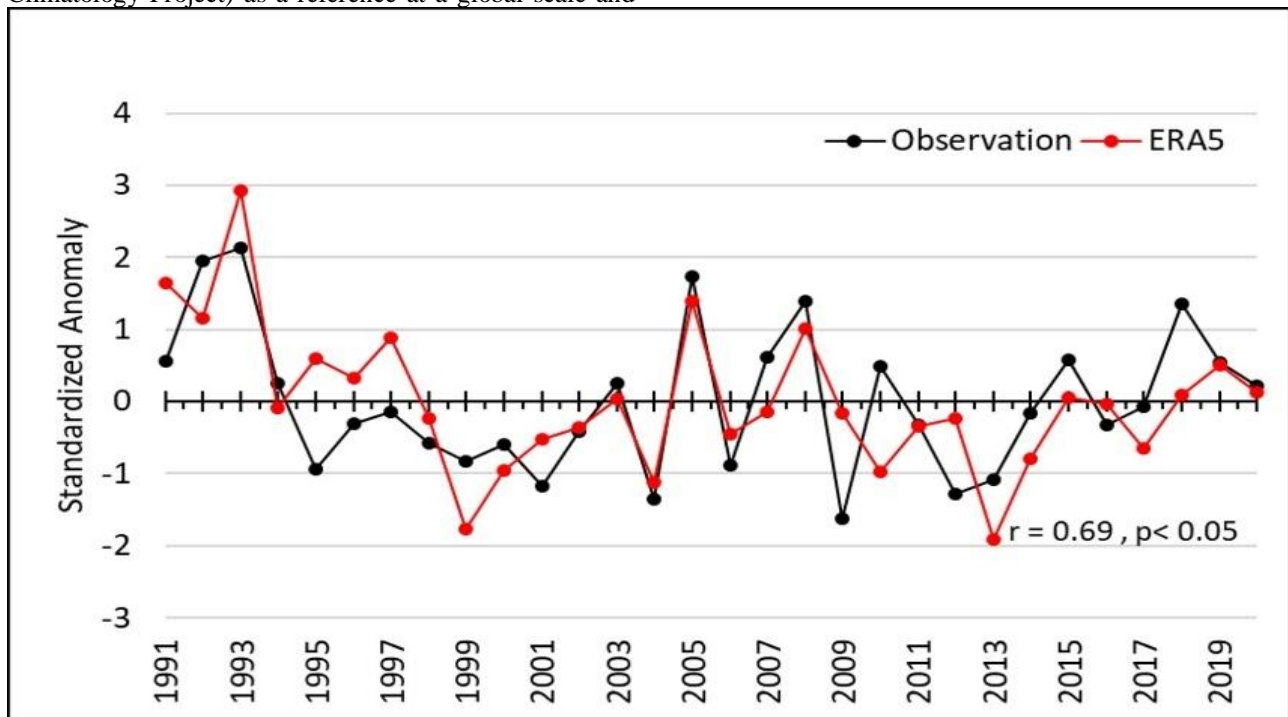

Figure 2: Validation of ERA5 Reanalysis data with 25 meteorological data from DMH (Myanmar)

Correlation analysis is used to test the validation of ERA5 gridded data set with the data from 25 meteorological station data across Myanmar and showed a strong correlation of 0.70 in the same period (Figure 2).

Empirical Orthogonal Function (EOFs) is the second method used in this paper. This has become a usual method in investigating the spatial characteristics of climatological fields. The EOFs are defined as the eigenvectors of the covariance matrix derived from the

time series of the data field (Mie Sein et al., 2015). The time series linked to the initial two EOFs (PCs) are investigated concerning the temporal variability. The link between regional surface data and large-scale upper-air fields has been investigated through covariance maps computed using the first two PCs of winter rainfall over the 1991–2020 interval. EOF theories and the computation method was adapted from (Lorenz, 1956). The idea is to identify the main circulation patterns, which could influence winter rainfall variability. The correlation coefficients between the winter rainfall PCs and the circulation indices, identified through the covariance map techniques, were also computed.

Correlation analysis and the determination of principle components (PCs), among other techniques, can be used to extract teleconnection patterns. There are some advantages to both methods in climate research, and both are widely used (Hamal et al., 2020). The composite analysis gives information about the common features and patterns of the variable in the atmosphere (Chen & Kumar, 2018). The statistical significance test of composite analysis in this study is determined using the student t-test at a 95% confidence interval. Numerous studies have presented the application of this analysis over the South Asian countries (Aung et al., 2017; Krishnamurthy & Shukla, 2000; Dimri et al., 2015). In this study, the Pearson correlation analysis aims at displaying the relationship between the variables at a 95% confidence level. The time series of all the climatic parameters were standardized detrend before going through EOF, composite, and correlation analysis.

3. Results and discussion

The monthly rainfall climatology over Upper Myanmar was analyzed using the ERA5 reanalysis data set during 1991–2020 (Figure 3.A). The analysis exhibited that the rainfall is highest within the rainy season and also the lowest within the winter season (DJF). The climatology of winter rainfall over Upper Myanmar is presented in (Figure 3.B). The mean winter rainfall is 10.03 mm/month during the study period. The winter rainfall is higher (above 25 mm/month) in the far-northern region than in southern and central regions (about 10–15 mm/month) of Upper Myanmar. A significant amount of WDs activity can be observed over Upper Myanmar during the peak winter months (DJF), and the Subtropical Westerly Jet (SWJ) can sometimes reach as far south as Middle Myanmar. Also, monthly average horizontal wind speed intensity is strongest in winter and decreases in spring (Dimri et al., 2015). The SWJ bringing winter rainfall is pronounced in the northern region and weakens from north to south.

Dominant Modes of rainfall variability over Upper Myanmar are presented in (Figure 4). Upper Myanmar is sustaining more or less rainfall-supported EOF maps; however, it produces variation of rainfall with eigenvalues. As part of the variance, the leading EOF1 mode represents 49.4%, and the leading EOF2 mode is

17.5%. Moreover, EOF1 indicates one mode of variability, with fairly high loadings in the northern regions (Figure 4.A). EOF2, on the other hand, exhibits a complex pattern (positive-negative-positive, from north to south) (Figure 4.B), with contradicting signals of variability in the far north and elsewhere. The distribution of rainfall in Upper Myanmar varies spatially due to local scale parameters, like orography, exposure, and also the direction of the range of mountains (Zaw et al., 2021).

The specific principal components (PC1 and PC2) of EOF1 and EOF2 are presented in (Figure 5.A, B), respectively. The PC1 and PC2 indicated the interannual and decadal variation of rainfall over Upper Myanmar from 1991 to 2020. PC1 statistics exhibit decadal variability of rainfall, from a positive first decadal anomaly of rainfall (1991–2020) has changed to a negative anomaly during the last two decades (2001–2020) over Upper Myanmar (Figure 5.A). This means that in these decades, the spatial distribution of rainfall was reversed mainly within the far northern and southern regions (Figure 5.A). The exceeding value of PC2, i.e., standardized anomalies exceeding +/- 1, shows the below or above-average rainfall and contrariwise (Figure 5.A). Thus, 1991, 1993, 1995, 1997 and 2005 are above-normal precipitating years, contrarily 1999, 2010, 2013 and 2017 are below-normal rainfall years.

Table 1: Two correlation modes of EOF and winter rainfall

EOF	Correlation
EOF1	0.9 (p<0.05)
EOF2	-0.3 (p=0.1)

The variability of interannual winter rainfall and PC1 over Upper Myanmar between 1991 and 2020 is presented in Figure 6. It was found that EOF1 and standardized average winter rainfall over Upper Myanmar during 1991-2020 had a strong correlation coefficient (0.92) (Table 1). The EOF1 and PC1 modes have the maximum variance and are therefore best suited for describing the winter rainfall variability in Upper Myanmar over the research period. The temporal analysis revealed that the study area experienced a below-average rainfall amount between 1998, 1999, 2000, 2001, 2002, 2004, 2007, 2008, 20010, 2011, 2013, 2014, 2015, 2016, 2017, and 2018. The anomalies of strong and weak years were chosen based on standardized anomalies by threshold ± 1 (Figure 6). The result shows each positive (strong: 1991, 1993, 1995, 1997, and 2005) and negative (weak: 1999, 2010, 2013, and 2017) anomaly year.

The composites of rainfall anomalies during wet and dry years are shown in (Figure 7). The wet year composite (Figure 7.A) has significant positive anomalies all over the study area with weak negative loading in the southeastern region, which corresponds with the dominant mode of EOF1, as in (Figure 4 A). The converse pattern was observed in the dry years (Figure 7. B). In addition to this synoptic-scale system, we have also winter westward

disturbances (WDs), embedded in the subtropical westerly jet (SWJ). To understand climatology values of OLR, the vertical velocity at 500hPa, wind vector and strength at 850hPa, and vertical moisture flux transport of 1000hPa to 200hPa what associated with WDs are shown in Figure 8. A, B, C, and D respectively. Then, 2m air temperature, relative humidity at 850hPa, 200hPa geopotential height and mean sea level pressure values are also shown in Figure 9. A, B, C, and D respectively.

Figure 10.A, B was produced to show a composite of OLR of dry and wet years. Rainfall has an enough linked reverse relation with OLR in both tropical and sub-tropical regions (Shen et al., 2017). In a wet (dry) year, positive (negative) anomalies OLR are observed over Myanmar, Cambodia, Vietnam, and south China sea regions to comprehend the cause for positive and negative anomalies of rainfall over Upper Myanmar. Likewise, during wet (dry) years, positive (negative) OLR was seen across the Bay of Bengal region and the South China Sea region, respectively. The low (high) values of OLR indicate higher (lower) cloud tops and resulting more (less) rainfall in the wet (dry) years (Lim et al., 2011). Additionally, vertical velocity explains the sinking and rising characteristics of clouds (Thériault & Stewart, 2007). The composite of vertical velocity anomalies at 500 hPa for the wet and dry years is presented in Figure 10.C, D. Negative anomalies have been found in Upper Myanmar, southwestern China, northern India, and southern parts of South China sea in wet years. As contrast, positive anomalies during dry years. This pattern is clear over the far north of Upper Myanmar (Myanmar, China, and India boundary region). There are notable positive vertical velocity anomalies at 500 hPa over this area (26–30∘N,95–100∘E) favoring a strong convective motion, pointing toward enhanced rainfall amount (Figure 10C). The reverse pattern was found in dry years, i.e., positive anomalies of vertical velocity over the study region; proper for subsidence which results in less rainfall (Figure 10.D). The negative values of vertical velocity increase the convective activity and produce a significant area of rainfall (Ahmed et al., 2020).

The WDs are speedy air-currents that can get amplified and developed by the topography and orography of South Asia (Lang & Barros, 2004). They are traveling to Upper Myanmar following the route of Iran, Afghanistan, Pakistan, Nepal, and north India. The westerlies wind run as a significant role in carrying and supplying moisture to the shifting of WDs (Dimri, 2013). Figure 11.A, B presents the zonal and meridional components wind vector and intensity at 850 hPa during the wet and dry years, respectively. The analysis appears that the stronger southwesterly wind anomalies are relative with a rainfall increase in Upper Myanmar and northern India during wet years (Figure 11. A). Figure 11.B shows reverse characteristics, indicating a strengthening of the northeasterly wind vectors during the dry years. By contrast, the wind vector patterns at 850 hPa, it is obvious that cyclonic circulation rest at 110–115∘E 3–7∘N during wet years.

Besides, Figure 11.C, D represents the vertically integrated moisture transport and wind vectors during wet and dry years measured from surface pressure level (1000 hPa) to the top of the atmosphere (200 hPa) in this study during 1991–2020. The moisture transport during wet and dry cases can be found a clear difference in magnitude, the direction of the wind, and a way of moisture transport to the study area. The positive anomalies of moisture (divergence) are found over the study region in the dry years, (Figure 11. C). Indifference, the negative anomalies of moisture (convergence) are found clearly over the study region (Figure 11.D). West China and the southern side of South China sea regions also show intense convergent/divergent fluxes. An anomalous anticyclonic (cyclonic) circulation persists over the southern part of the Bay of Bengal and South China sea (around 90–100∘E, 2–10∘N) during wet (dry) years (Figure 11C, D). The previous study stated that such circulations strong (weak) the supplements of moisture from nearby seas in the study region (Dimri, 2013).

Air temperature is an applicable useful parameter for determining extreme conditions. the strong negative anomalies are observed over Southern China regions, Delta and Upper regions of Myanmar during the wet years (Figure 12. A)., and as reverse, the strong positive anomalies of air temperature are observed over same regions during dry years (Figure 12. B). In contrast, the northern India region (around 80–90∘E, 24–28∘N) shows strong positive anomalies in wet years and negative in dry years advance. Similarly, recent research in the Himalayas discovered a link between winter rainfall and air temperature that was negative (Dimri, 2014). Both the Himalayas and the TP regions are resting in an important role for the modification of the westerly system and moisture transport (Ahmed et al., 2020). The warming over the Indian Ocean and the cooling over the Tibetan plateau region correspond to south-north transport of moisture, ensuing in positive rainfall anomalies over the study region during winter (Figure 7. B).

The findings of this study agree well with those of a previous study (Dimri, 2014). Furthermore, in different seasons, the heating and cooling of the Tibetan plateau can impact air circulation and large–scale teleconnections. The increase in summer rainfall and decreasing winter rainfall trends are observed in Upper Myanmar because of the accelerated increasing warming trend of annual temperature over Myanmar (K. K. Sein et al., 2018). Moreover, the positive anomalies of relative humidity at 850 hPa largely predominately north to south in the study area during the wet years (Figure 12. C). In dry years, negative humidity anomalies are results over Upper Myanmar (Figure 12.D).

In the research location, the patterns of humidity and temperature are inversely connected during dry years and slightly reverse during wet years. It means that colder (warmer) temperatures are frequently accompanied by dry (wet) weather. The temperature variability over the TP also has a strong relation with winter rainfall over Upper Myanmar.

Numerous recent studies highlight a wide part of the climate and weather predictability linked to the ocean, while the spatial patterns of the effects of such global teleconnections as IOD and ENSO, along with the local SSTs on winter rainfall (S. Sen Roy, 2006). The ENSO indication of atmospheric variability has been studied comprehensively and is believed to function as an ''atmospheric bridge'' that links interannual SST fluctuations in the tropical Pacific with oceanic variations at higher latitudes (Alexander et al., 2002; Nga Lau and Nath, 1994). From previous winter SST correlation with rainfall over Upper Myanmar shows moderate negative (positive) correlation at the north (south) of equatorial (20°N –20°S). Although, NINO 3-4 (5°N-5°S and 170°W-120°W) region has a positive correlation with other equatorial regions (Figure 13). In contrast, a Strong negative correlation can also be seen over the North and South Pacific Ocean (NPO, SPO), Mediterranean Sea (MDS), Red Sea (RDS), and Bay of Bengal (BOB). The lagged correlation between the average trend of winter rainfall and SST for 30 years (1991– 2020) (Figure 13) is produced based on interannual variability (Figure 6), to Observe the dependence of winter rainfall on each lagged year on large-scale global forces. The area of significant correlation positive (negative) resulted for wet, dry, and rest normal years (Figure 14. A, B, C).

The wide patches of strong negative (positive) correlation are found over the Pacific Ocean, the Atlantic Ocean, Mediterranean Sea (MED), Arabian Sea (ARS), and Red Sea (RED) during wet (dry) years (Figure 14.A, B). Furthermore, from the previous winter onwards, a positive correlation (warming) with ARS (10°N-25°N and 55°E to 75°E) SST during wet (dry) years (Figure 14.A, B). In contrast, a negative correlation (cooling) with the MDS, NPO, SPO during wet(dry) (Figure 14. A, B). years. However, a significant correlation is slightly weak only during the rest of the years (Figure 14. C). The finding is quite interesting as NPO, SPO, ARS, and MED may have an impact on the winter rainfall of Upper Myanmar (Figure 14). The results also demonstrate that less winter rainfall over Upper Myanmar is linked with higher-than-average SST in the MED and western PO (Figure 14. B).

It suggests that during the warm phase of ENSO, more rainfall can be expected due to enhanced southwesterly winds. The wind circulation pattern (Figure 11. A, B) is forced during La Nina (El Nino) events; that involves southwesterly (northeasterly) moisture transport (Figure 11. C, D) which brings above (below) normal rainfall (Figure 7.A, B) over the study region (Mariotti & Dell'Aquila, 2012). Also, ENSO influences the vertical baroclinic reaction over the TP (as shown in Figure 10. C,D), which encourages the WDs activities (Dimri, 2014; Yadav et al., 2009).

As climatology, to winter rainfall for the period of 1991 to 2020 is the moderate negative correlation between SPO (r = -0.55, p <0.001) and RED (r = 0.06, p<0.01). For positive correlation, only NINO (r = -0.09, p = 0.08) with winter rainfall during the study period. The concurrent response of MED is negative, and it has a strong significant correlation of ~0.8 in both wet (p=0.11) and dry (p=0.38) years (Table 2). MED is a clear indicator for the forecast of the following year's winter rainfall over Upper Myanmar. However, the rest years (nearly normal) also has a negative correlation with weak significant (r = -0.2, p = 0.52) than above mentioned that the positive (negative) mode of MED is favorable (unfavorable) for rainfall over the study area. For the mean result, MED has a moderate negative correlation (r = -0.35, p = 0.06) with winter rainfall over Upper Myanmar.

The result advises that warming of the Indian Ocean can extend or gap the influence of ENSO on winter rainfall (Yang et al., 2007). Besides, the increased rainfall over the study area is associated with below-normal SST in the equatorial Pacific and the Indian Ocean, which elevated the reaction of the Hadley and Walker Circulation (Dimri, 2006). The warming SST over the Atlantic and the Indian Ocean increases the convention over the region that helps in fluctuating the Subtropical Westerly Jet (SWJ) over the Indian continent (Yadav et al., 2012). The existence of the divergence at 200 hPa over equatorial IO and northwestern of PO (Figure 15.A) helps in bringing moisture from the MED and Arabian Sea (ARS) and supporting the migratory of WDs. Moreover, the heating over IO and cooling over TP (Figure 12.B) correspond to the north-south transfer of moistures to the study region. These actions result in dry years which are reversible for the wet years.

The main study is that the interannual variability of winter rainfall in Upper Myanmar was correlated with global SST warming and cooling. Especially, PO and MED including NINO. Furthermore, more (less) rainfall can be expected in La Niña (El Niño) phases of NINO with DMI negative. The drought events are increasing in Upper Myanmar, mainly after 2000 (Wang et al., 2013). Therefore, the Walker circulation over the PO and IO for dry years (El Niño years) is present in Figure 15.B. The pattern observed in the given figures indicates that the equatorial Indo-pacific walker circulation is affected by ENSO. SSTs over eastern Atlantic Oceans and western Pacific are negatively correlated with wet years, while those over eastern Pacific and maritime continents are positively correlated with wet years. The three cell Walker circulations were noticed over the tropical Indian Ocean (IO) and Pacific Ocean (PO), with two descending regions over the IO and the western PO maritime continent and one ascending region over the western PO respectively in wet years (Figure 15.A). Further, it also displays the upper-level convergent of wind anomalies over the western PO and divergence over the east IO maritime continent and the eastern PO maritime continent during dry years (Figure 15.B). The cooling occurs in the Tibetan Plateau (TP) region during wet years (Figure 12.A), showing the upper-level convergence of wind anomalies (around 30°N 90°E, Figure 15). The pattern counteracts a reaction of Walker circulation over the Indian and Pacific regions. The sinking (descending) atmospheric motion over the IO and the rising (ascending) motion over the TP have weakened the Hadley circulation (Figure 15.B) resulting in the dry years.
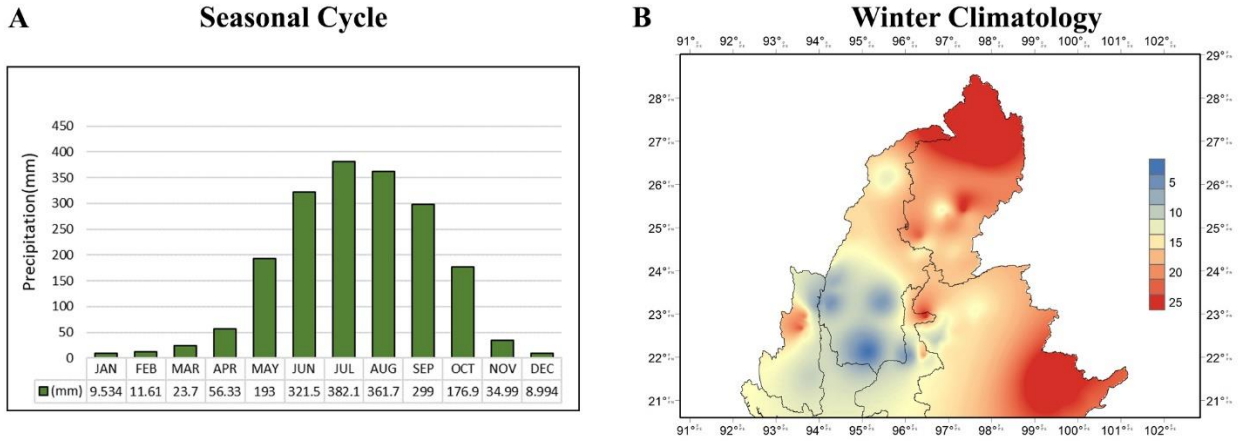
Figure 3: (A) Seasonal cycle and (B) Climatology of winter precipitation (mm/month) over Upper Myanmar from 1991 to 2020
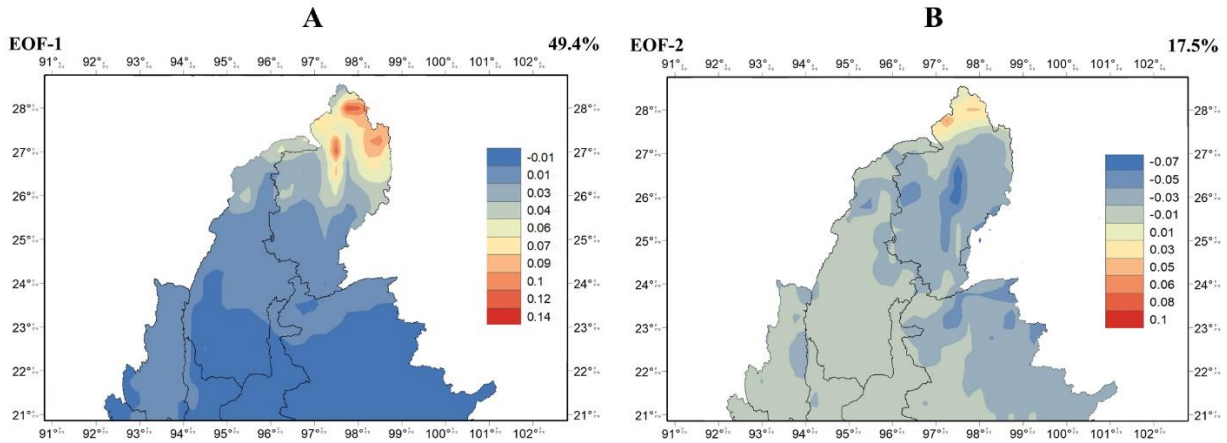

Figure 4: (A) The first dominant mode of variability (EOF1) explains 49.4% of the total variance of the mean winter precipitation and (B) the second dominant mode of variability (EOF2) explains 17.5% of the total variance of the mean winter precipitation over upper Myanmar.
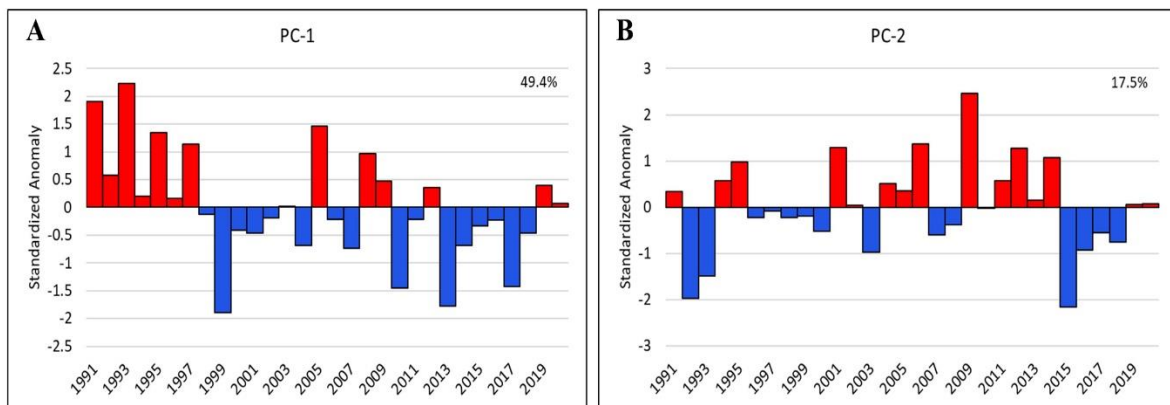

Figure 5: (A) The first Principal Component associated with EOF1 (PC1) and (B) The second Principal Component associated with EOF2 (PC2) of winter rainfall over Upper Myanmar, based on ERA5 data from 1991 to 2020
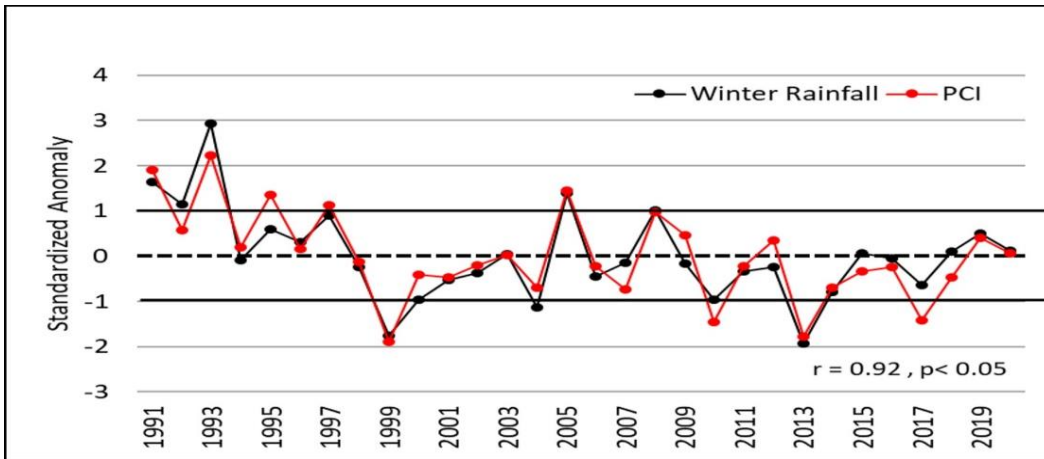
Figure 6: Inter–annual variability of PC1 and winter precipitation anomaly over Upper Myanmar. The black dotted line represents the reference line and blackline separates the wet and dry years during 1991–2020
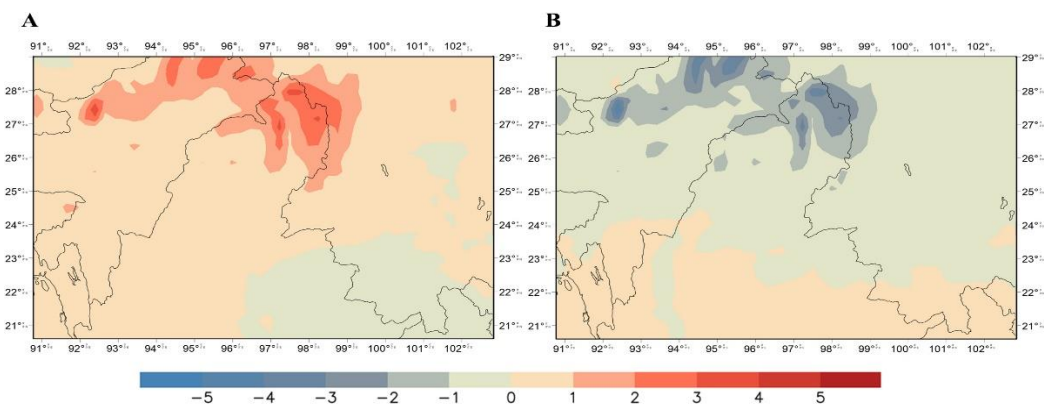
Figure 7: Composite precipitation anomalies (mm/month) for (A) Wet years and (B) Dry years based ERA5 data between 1991 and 2020 with the significance at a 95% confidence level.
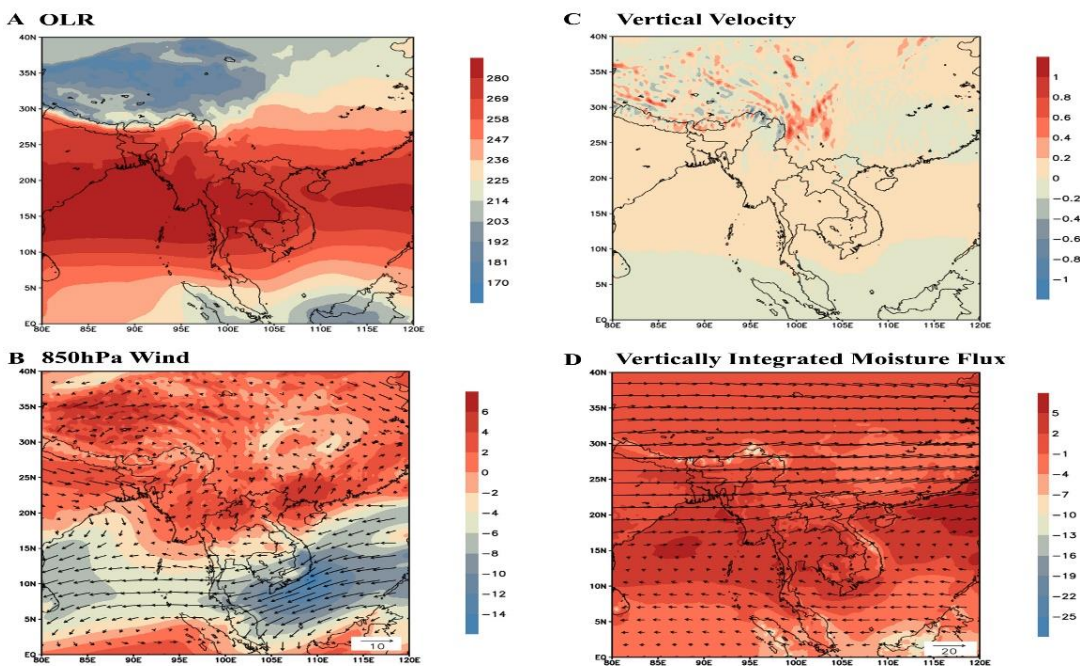
Figure 8: Composite Climatology (DJF) of (A) OLR anomalies (W/m2), (B) Wind vectors (ms−1) at 850hPa (shading indicates the zonal component of wind, (C)Vertical velocity (Pas−1) at 200hPa, (D) Vertically Integrated Water Moisture Flux (kg m−2 s−1) based on ERA5 data from 1991 to 2020
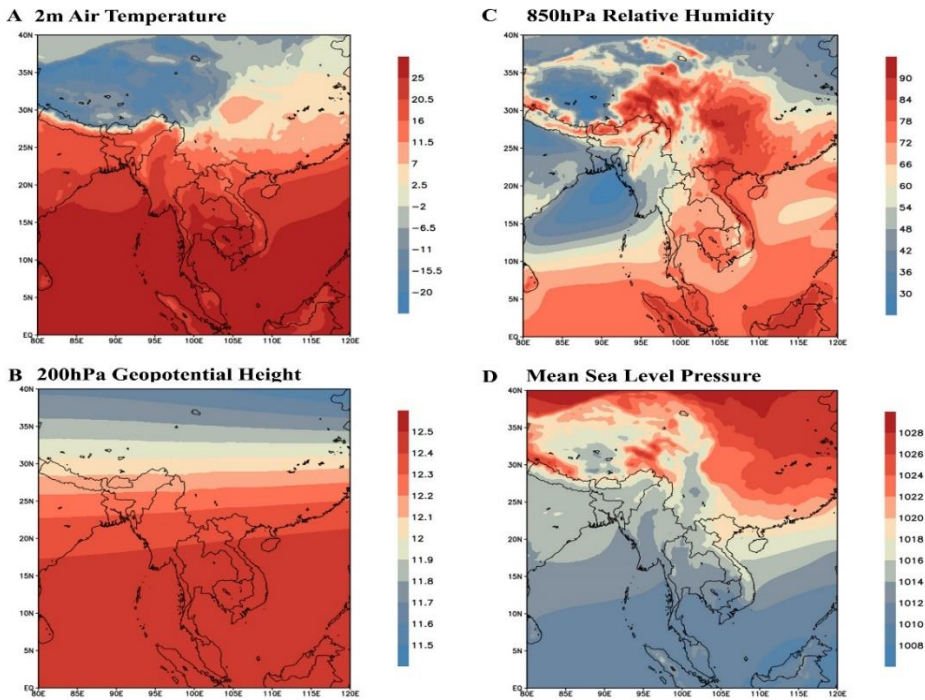
Figure 9: Composite Climatology (DJF) of (A) 2 m surface air temperature (◦C), (B) Geopotential Height at 200hPa (km), (C) humidity (%) at 850hPa, (D) Mean Sea level Pressure (hPa) based on ERA5 data from 1991 to 2020
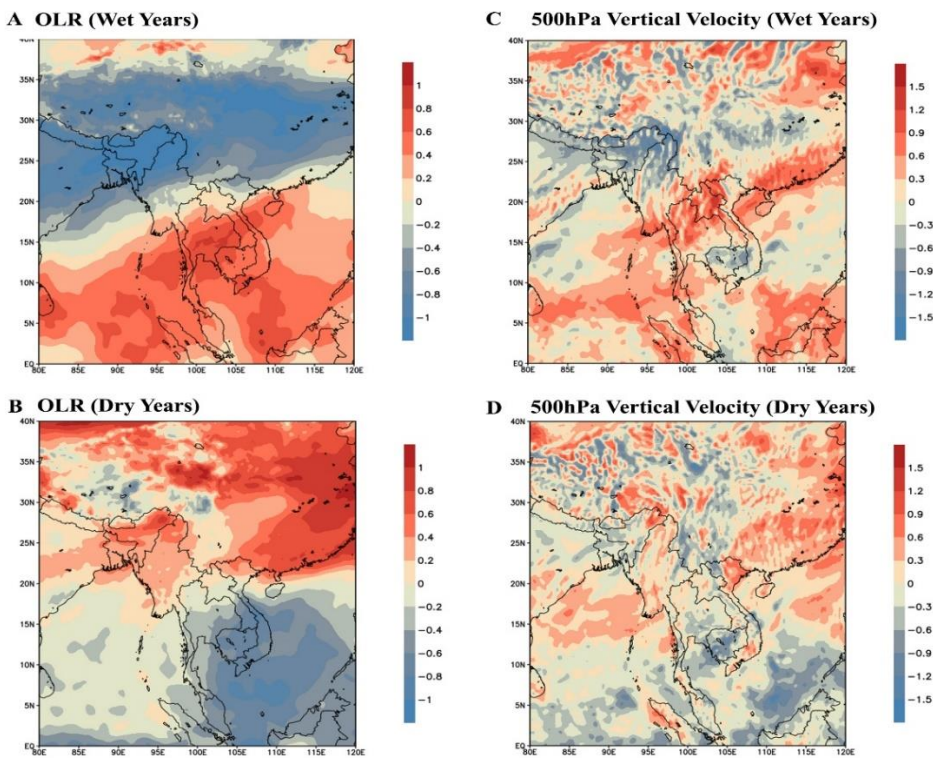
Figure 10: Composite OLR anomalies (10−5, W/m2) for (A) wet years, (B) dry years, and Vertical velocity (10, Pas−1) for (C) dry years, and (D) wet years based on ERA5 reanalysis data during 1991–2020.
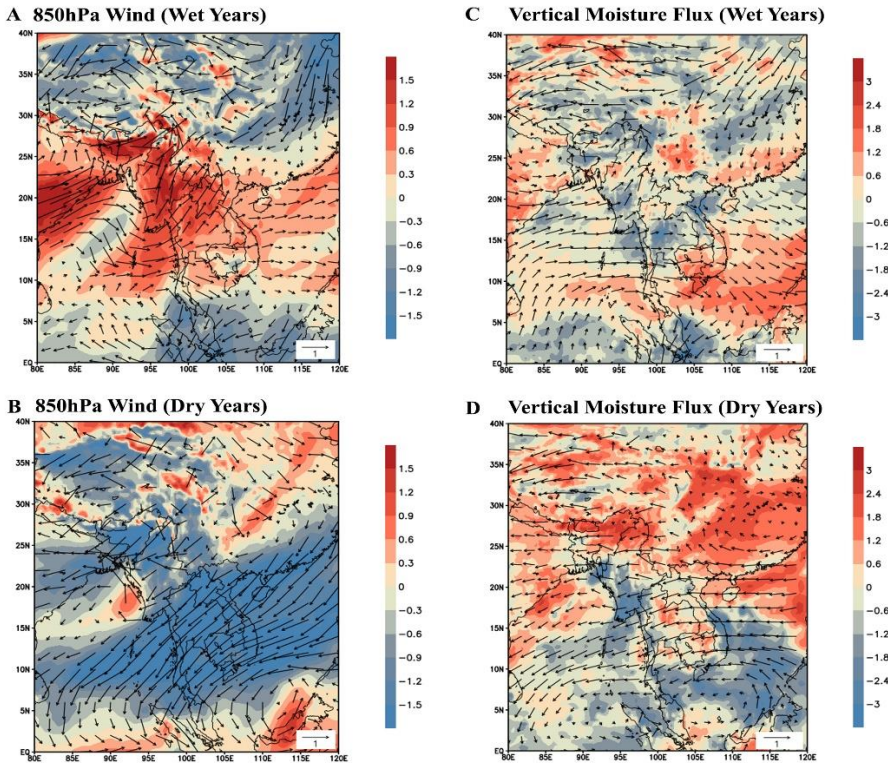
Figure 11: Wind vectors anomalies (ms^{-1}) at 850 hPa (shading color shows the zonal component of wind anomalies) for **(A)** wet years, **(B)** dry years. Vertically Integrated Water Vapors Flux (kg m^{-2} s^{-1}) shading color shows negative (convergence) and positive (divergence) anomalies for **(C)** wet years, and **(D)** dry years from 1991 to 2020.

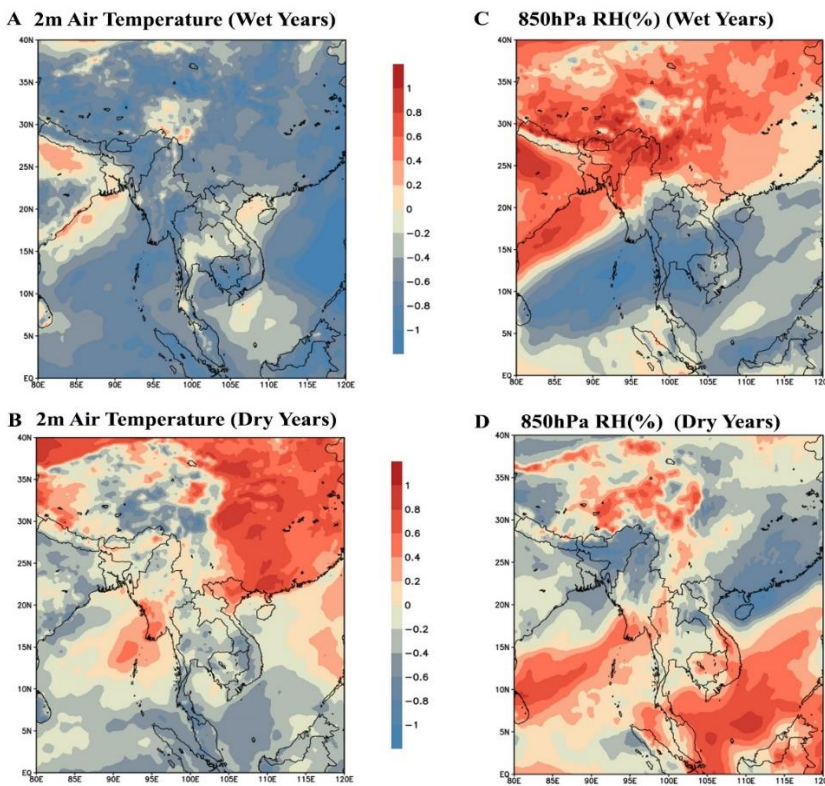**Figure 12:** Composite anomalies of 2 m surface air temperature (∘C) for (A) wet years, (B) dry years, and relative humidity (10−1, %) during (C) wet years, (D) dry years based on ERA5 reanalysis data from 1991 to 2020
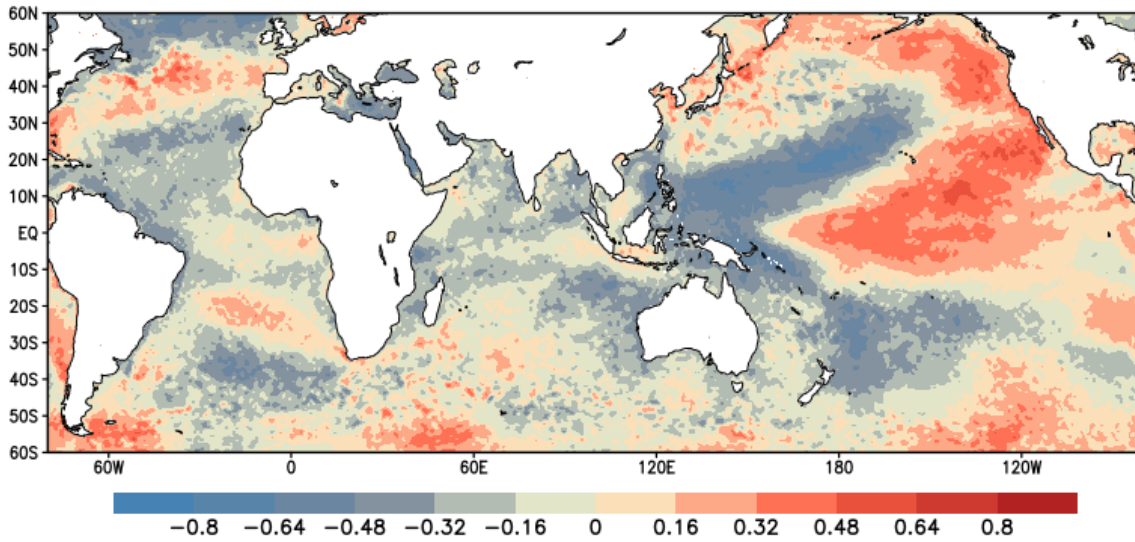
Figure 13: Correlation of winter SST with winter precipitation over Upper Myanmar (1991-2020)
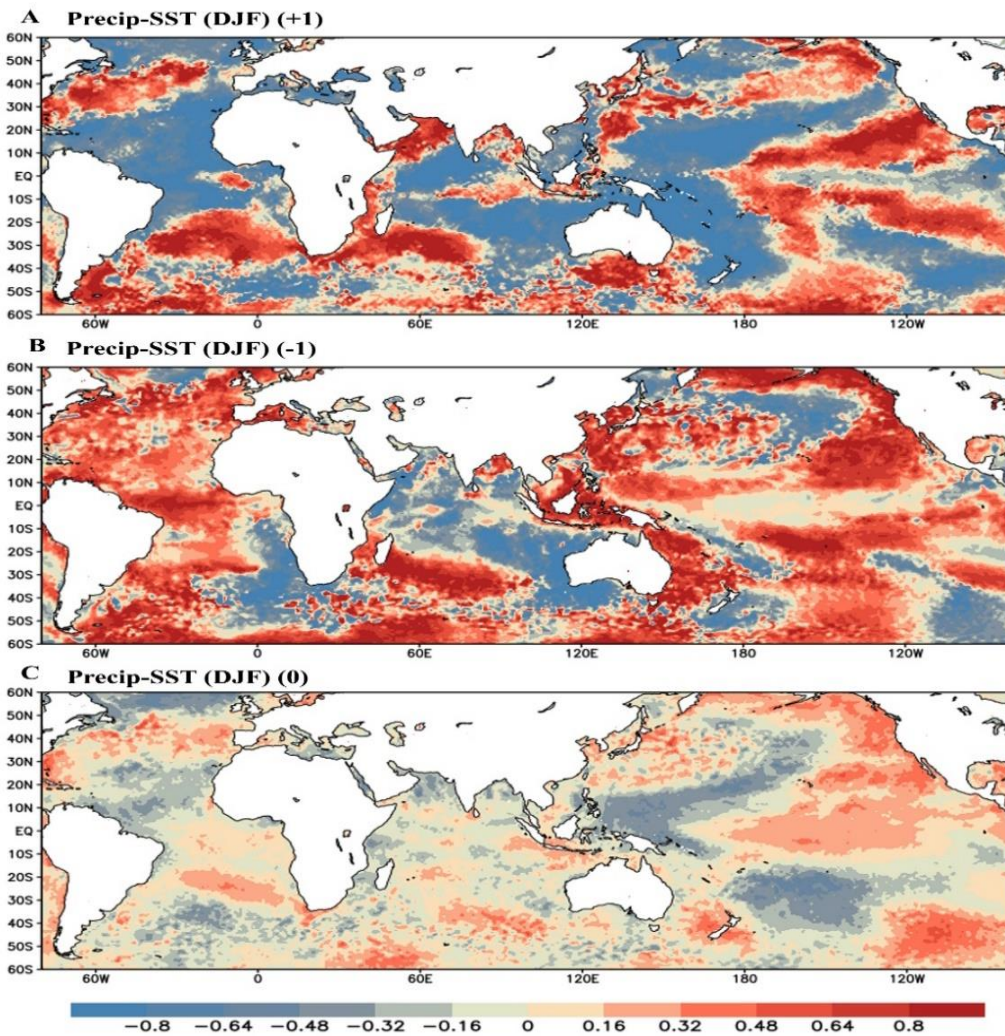

Figure 14: Correlation between averaged winter precipitation and SST during 1991–2020 (A) Wet Year (+1), (B) Dry Year (−1), (C) Rest normal years (0), respectively. +1,−1 and 0 represents lag and corresponding winter precipitation anomaly as in Figure 6.
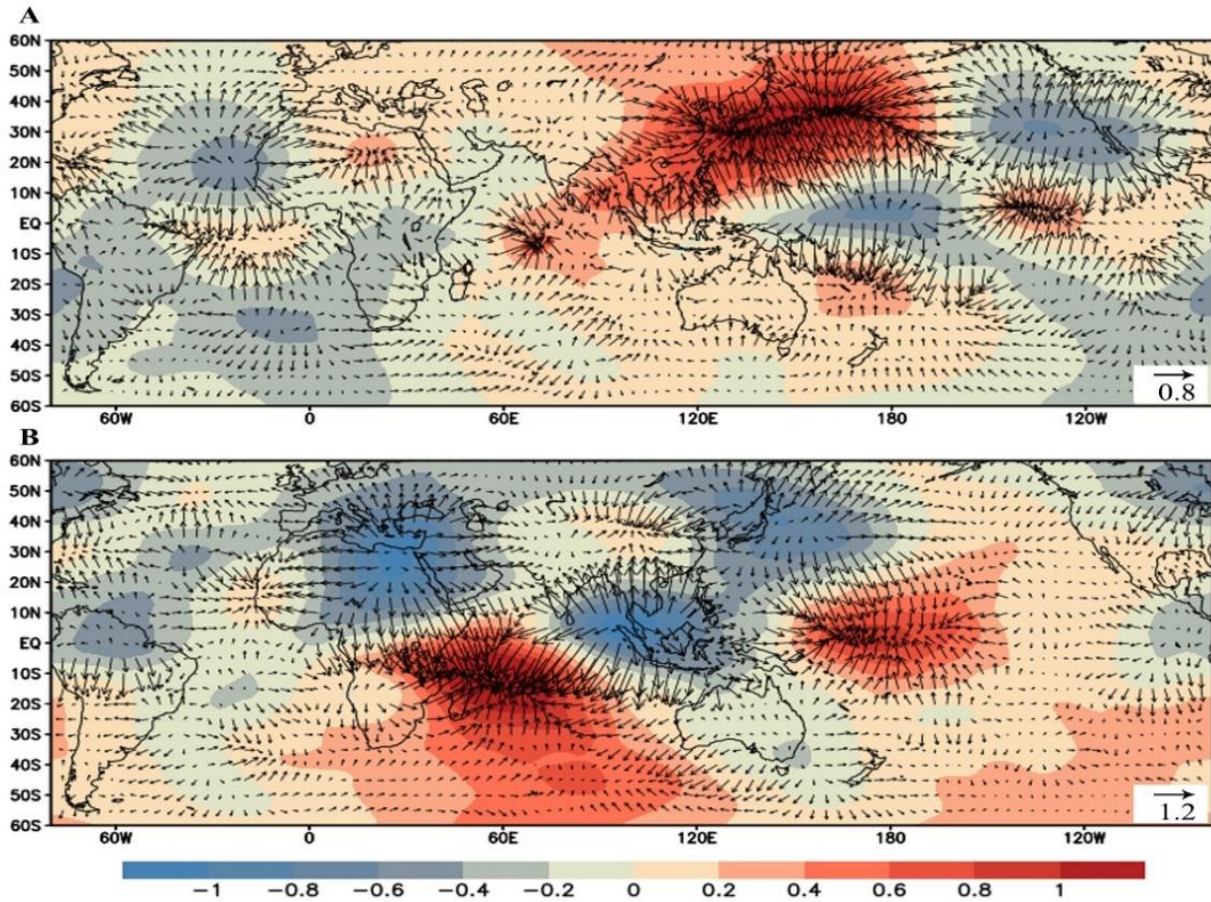
Figure 15: 200 hPa divergent/convergent winds (vectors; m2 s−1) and velocity potential (contours; 10−6, m2 s−1) for (A) wet years, (B) dry years based on ERA5 reanalysis data from 1991 to 2020.

Table 2: Lagged correlation between winter rainfall with NINO, NAD, DMI, PO, BOB, MED, and RED based on Figure 6.

Index	DJF(Normal)	DJF(Wet)	DJF(Dry)	DJF(Zero)
NINO	0.09 (p=0.64)	-0.40 (p=0.50)	0.21 (p=0.79)	0.08 (p=0.72)
NPO	-0.33 (p=0.08)	**-0.67 (p=0.22)**	**0.67 (p=0.33)**	-0.03 (p=0.89)
SPO	**-0.55 (p<0.01)**	-0.54 (p=0.34)	0.36 (p=0.64)	**-0.53 (p=0.01)**
IOBM	-0.29 (p=0.12)	**-0.61 (p=0.27)**	-0.34 (p=0.66)	-0.06 (p=0.79)
DMI	-0.13 (p=0.50)	-0.28 (p=0.65)	**-0.89 (p=0.11)**	-0.19 (p=0.42)
NAD	**-0.49 (p<0.05)**	-0.48 (p=0.41)	0.11 (p=0.89)	**-0.44 (p=0.05)**
BOB	-0.29 (p=0.12)	-0.05 (p=0.93)	0.31 (p=0.69)	-0.18 (p=0.44)
MED	-0.35 (p=0.06)	**-0.80(p=0.11)**	**0.62 (p=0.38)**	-0.15 (p=0.52)
RED	**-0.60 (p<0.01)**	-0.50(p=0.39)	-0.17 (p=0.83)	**-0.45 (p<0.05)**
ARS	-0.29 (p=0.12)	**-0.94(p<0.05)**	**0.54 (p=0.46)**	-0.29 (p=0.21)

4. Conclusion

This study examined the inter-annual variability of winter (DJF) rainfall over Upper Myanmar during the previous years from 1991 to 2020, linked with the ocean-atmosphere patterns. A high-resolution ERA5 reanalysis dataset is used to investigate the EOF, Correlation, and Composites analysis, respectively. Upper Myanmar sustains a very small amount of rainfall (about 2%) in winter. EOF analysis showed two dominant modes, likewise, the leading mode captures 49.4% of the total variance displayed a single mode of variability. The standardized anomalies of winter rainfall showed deficiency rainfall in 1999, 2010, 2013, and 2017, whereas, surfeit rainfall in 1991, 1993, 1995, 1997, and 2005. The results displayed negative (positive) anomalies of vertical velocity and OLR over Upper Myanmar during wet (dry) years. During dry years, moisture divergence is dominated by positive anomalies associated with northeasterly winds, whereas divergence is dominated by negative anomalies associated with southwest winds. The decrease in surface air temperature over the Asian highest continent (TP) leads to convergence of upper-level wind anomalies and western PO that impact the surfeit of winter rainfall. Furthermore, the positive SST over the NAD, MED, and PO suppressed the convective activity, which reduced the moisture transport to the Himalayan region, resulting in dry years. The association implies that NPO, SPO, and MED have an impact on the winter rainfall's inter-annual variability. In addition, the cooling (warming) over the Indochina and Tropical Pacific regions influences the Hadley and Walker circulation bringing above (below) normal rainfall, respectively, over Upper Myanmar. The subtropical westerly jet is also home to winter western disturbances (WDs). Upper Myanmar is broken at intervals by a series of WDs which travel Eastwards across Northern Upper Myanmar. The reply of indices (PO, MED, NINO3.4, IOD, and WDs) on winter rainfall, necessary to further study. Using comprehensive analyses of winter rainfall over Upper Myanmar to create forecasts and monitoring systems for droughts and floods, we can better understand past extreme events.

Acknowledgements

References

Ahmed, F., Adnan, S., & Latif, M. (2020). Impact of jet stream and associated mechanisms on winter precipitation in Pakistan. *Meteorology and Atmospheric Physics, 132*(2), 225–238. https://doi.org/10.1007/s00703-019-00683-8

Alexander, M. A., Bladé, I., Newman, M., Lanzante, J. R., Lau, N. C., & Scott, J. D. (2002). The atmospheric bridge: The influence of ENSO teleconnections on air-sea interaction over the global oceans. *Journal of Climate, 15*(16), 2205–2231. https://doi.org/10.1175/1520-0442(2002)015<2205:TABTIO>2.0.CO;2

Aung, L. L., Zin, E. E., Theingi, P., Elvera, N., Aung, P. P., Han, T. T., Oo, Y., & Skaland, R. G. (2017). Myanmar Climate Report. *Norwgian Meterological Institute, 9*, 105.

Bjerknes, J. (1969). Monthly Weather Reyiew Atmospheric Teleconnections From the Equatorial Pacific. *Monthly Weather Review, 97*(3), 163–172. http://journals.ametsoc.org/doi/abs/10.1175/1520-0493(1969)097%3C0163:ATFTEP%3E2.3.CO;2

Cannon, F., Carvalho, L. M. V., Jones, C., & Bookhagen, B. (2015). Multi-annual variations in winter westerly disturbance activity affecting the Himalaya. *Climate Dynamics, 44*(1–2), 441–455. https://doi.org/10.1007/s00382-014-2248-8

Chen, M., & Kumar, A. (2018). Winter 2015/16 atmospheric and precipitation anomalies over North America: El Niño response and the role of noise. *Monthly Weather Review, 146*(3), 909–927. https://doi.org/10.1175/MWR-D-17-0116.1

Dimri, A. P. (2006). Surface and Upper Air Fields During Extreme Winter Precipitation Over the Western Himalayas. *Pure and Applied Geophysics, 163*(8), 1679–1698. https://doi.org/10.1007/S00024-006-0092-4

Dimri, A. P. (2013). Relationship between ENSO phases with Northwest India winter precipitation. *International Journal of Climatology, 33*(8), 1917–1923. https://doi.org/10.1002/joc.3559

Dimri, A. P. (2014). Sub-seasonal interannual variability associated with the excess and deficit Indian winter monsoon over the Western Himalayas. *Climate Dynamics, 42*(7–8), 1793–1806. https://go.gale.com/ps/i.do?p=AONE&sw=w&issn=09307575&v=2.1&it=r&id=GALE%7CA380747281&sid=googleScholar&linkaccess=fulltext

Dimri, A. P., Niyogi, D., Barros, A. P., Ridley, J., Mohanty, U. C., Yasunari, T., & Sikka, D. R. (2015). Western Disturbances: A review. *Reviews of Geophysics, 53*(2), 225–246. https://doi.org/10.1002/2014RG000460

FAO, & AVSI Foundation. (2019). *Climate Smart Agriculture in Myanmar.*

Hamal, K., Sharma, S., Baniya, B., Khadka, N., & Zhou, X. (2020). Inter-Annual Variability of Winter Precipitation Over Nepal Coupled With Ocean-Atmospheric Patterns During 1987–2015. *Frontiers in Earth Science, 8.* https://doi.org/10.3389/feart.2020.00161

Horel, J.D. (1981). *Planetary-scale atmospheric phenomena associated with the interannual variability of sea surface temperature in the equatorial Pacific.*

Jiao, D., Xu, N., Yang, F., & Xu, K. (2021). Evaluation of spatial-temporal variation performance of ERA5 precipitation data in China. *Scientific Reports, 11(*1), 1–13. https://doi.org/10.1038/s41598-021-97432-y

Karoly, B.J.H. (1981). *The steady linear response of a Spherical Atmosphere to Thermal and Orographic Forcing.*

Krishnamurthy, V., & Shukla, J. (2000). Intraseasonal and interannual variability of rainfall over India. *Journal of Climate, 13(*24), 4366–4377. https://doi.org/10.1175/1520-0442(2000)013<0001:IAIVOR>2.0.CO;2

Lang, T.J., & Barros, A.P. (2004). Winter storms in the central Himalayas. *Journal of the Meteorological Society of Japan, 82(*3), 829–844. https://doi.org/10.2151/jmsj.2004.829

Lim, E.S., Wong, C.J., Abdullah, K., & Poon, W. K. (2011). Relationship between outgoing longwave radiation and rainfall in South East Asia by using NOAA and TRMM satellite. *IEEE Colloquium on Humanities, Science and Engineering, 785–790.* https://doi.org/10.1109/CHUSER.2011.6163843

Lorenz, E.N. (1956). *Empirical orthogonal functions and statistical weather prediction.* In Technical report Statistical Forecast Project Report 1 Department of Meteorology MIT.

Lu, B., Li, H., Wu, J., Zhang, T., Liu, J., Liu, B., Chen, Y., & Baishan, J. (2019). Impact of El Niño and Southern Oscillation on the summer precipitation over Northwest China. *Atmospheric Science Letters, 20(*8), 1–8. https://doi.org/10.1002/asl.928

Mariotti, A., & Dell'Aquila, A. (2012). Decadal climate variability in the Mediterranean region: Roles of large-scale forcings and regional processes. *Climate Dynamics, 38(*5–6), 1129–1145. https://doi.org/10.1007/S00382-011-1056-7

Mie Sein, Z.M., Islam, A.R.M.T., Maw, K.W., & Moya, T.B. (2015). Characterization of southwest monsoon onset over Myanmar. *Meteorology and Atmospheric Physics, 127(*5), 587–603. https://doi.org/10.1007/s00703-015-0386-0

Nageswararao, M.M., Mohanty, U.C., Osuri, K.K., & Ramakrishna, S.S.V.S. (2016). Prediction of winter precipitation over northwest India using ocean heat fluxes. *Climate Dynamics, 47(*7–8), 2253–2271. https://doi.org/10.1007/s00382-015-2962-x

Ngar-Cheung Lau and Mary Jo Nath. (1994). *A modeling study of the relative roles of tropical and extratropical SST anomalies in the variability of the global atmosphere-ocean system.*

Oo, K.T., & Thin, M.M.Z. (2022). Climate Change Perspective: The Advantage and Disadvantage of COVID-19 Pandemic. *Journal of Sustainability and Environmental Management, 1(*2), 275-291.

Saji, N. H., Goswami, P. N., Vinayachandran, P. N., & Yamagata, T. (1999). Saji,N.A et al,.dipole mode in the tropical Indian ocean. *Nature, 401,* 360–363. http://www.nature.com/doifinder/10.1038/43854%0Apapers3://publication/doi/10.1038/43854

Sein, K. K., Chidthaisong, A., & Oo, K.L. (2018). Observed trends and changes in temperature and precipitation extreme indices over Myanmar. *Atmosphere, 9(*12). https://doi.org/10.3390/atmos9120477

Sein, Z.M.M., Ogwang, B., Ongoma, V., Ogou, F.K., & Batebana, K. (2015). Inter-annual variability of May-October rainfall over Myanmar in relation to IOD and ENSO. *Journal of Environmental and Agricultural Sciences, 4,* 28–36.

Sen Roy, N., & Kaur, S. (2000). Climatology of monsoon rains of Myanmar (Burma). *International Journal of Climatology, 20(*8),913–928. https://doi.org/10.1002/1097-0088(20000630)20:8<913::AID-JOC485>3.0.CO;2-U

Sen Roy, S. (2006). The impacts of ENSO, PDO, and local SSTS on winter precipitation in India. *Physical Geography, 27(*5), 464–474. https://doi.org/10.2747/0272-3646.27.5.464

Shen, Z., Shi, J., & Lei, Y. (2017). Comparison of the Long-Range Climate Memory in Outgoing Longwave Radiation over the Tibetan Plateau and the Indian Monsoon Region. *Advances in Meteorology.* https://doi.org/10.1155/2017/7637351

Thériault, J. M., & Stewart, R. E. (2007). On the effects of vertical air velocity on winter precipitation types. *Natural Hazards and Earth System Science, 7(*2), 231–242. https://doi.org/10.5194/nhess-7-231-2007

Tošić, I., Hrnjak, I., Gavrilov, M. B., Unkašević, M., Marković, S. B., & Lukić, T. (2013). Annual and seasonal variability of precipitation in Vojvodina, Serbia. *Theoretical and Applied Climatology, 117(*1), 331–341. https://doi.org/10.1007/s00704-013-1007-9

Wang, W., Zhou, W., Wang, X., Fong, S.K., & Leong, K.C. (2013). Summer high temperature extremes in Southeast China associated with the East Asian jet stream and circumglobal teleconnection. *Journal of Geophysical Research Atmospheres, 118(*15), 8306–8319. https://doi.org/10.1002/JGRD.50633

Xoplaki, E., González-Rouco, J.F., Luterbacher, J., & Wanner, H. (2004). Wet season Mediterranean precipitation variability: Influence of large-scale dynamics and trends. *Climate Dynamics, 23(*1), 63–78. https://doi.org/10.1007/s00382-004-0422-0

Yadav, R.K., Rupa Kumar, K., & Rajeevan, M. (2009). Out-of-phase relationships between convection over northwest India and warm pool region during the

winter season. *International Journal of Climatology, 29(*9), 1330–1338. https://doi.org/10.1002/JOC.1783

Yadav, R.K., Rupa Kumar, K., & Rajeevan, M. (2012). Characteristic features of winter precipitation and its variability over northwest India. *Journal of Earth System Science, 121(*3), 611–623. https://doi.org/10.1007/s12040-012-0184-8

Yang, J., Liu, Q., Xie, S.P., Liu, Z., & Wu, L. (2007). Impact of the Indian Ocean SST basin mode on the Asian summer monsoon. *Geophysical Research Letters, 34(*2). https://doi.org/10.1029/2006GL028571

Zaw, Z., Fan, Z.X., Bräuning, A., Liu, W., Gaire, N.P., Than, K. Z., & Panthi, S. (2021). Monsoon precipitation variations in Myanmar since AD 1770: linkage to tropical ocean‑atmospheric circulations. *Climate Dynamics, 56(*9 – 10), 3337 – 3352. https://doi.org/10.1007/s00382-021-05645-8

Zhou, X., Wang, W., Ding, R., Li, J., Hou, Z., & Xie, W. (2019). An investigation of the differences between the North American dipole and North Atlantic Oscillation. *Atmosphere, 10(*2). https://doi.org/10.3390/atmos10020058

Zin, E. E., Aung, L. L., Zin, E. E., Theingi, P., Elvera, N., Aung, P. P., Han, T. T., Oo, Y., & Skaland, R. G. (2017). Myanmar Climate Report. *Norwgian Meterological Institute,* 9, 105. http://files/679/MyanmarClimateReportFINAL11Oct2017.pdf

Zin, E. E., Aung, L. L., Zin, E. E., Theingi, P., Elvera, N., Aung, P. P., Han, T. T., Oo, Y., Skaland, R. G., & Aung, L. L.; Zin, E. E.;Theingi, P.;Elvera, N.; Aung, P.; Han, T.; Oo, Y.; Skaland, R. (2017). Myanmar Climate Report. *Norwgian Meterological Institute*, 9, 105. http://files/679/MyanmarClimateReportFINAL11Oct2017.pdf

.